Journal of Hyperbolic Differential Equations
Vol. 1, No. 2 (2004) 315–327

World Scientific
www.worldscientific.com

THE DYNAMICS OF PRESSURELESS DUST CLOUDS AND DELTA WAVES

RANDALL J. LEVEQUE
Applied Mathematics Department, Box 352420
University of Washington
Seattle, WA 98195-2420, USA

Received 11 Nov. 2003
Revised 18 Nov. 2003

Communicated by J.-G. Liu

Abstract. The equations of isothermal gas dynamics are studied in the limit when the sound speed vanishes, giving the so-called pressureless gas equations. The collision of two clouds of dust is modeled with these equations in the case where the clouds have finite extent and are surrounded by vacuum. The delta shock that arises in the initial stage of the collision evolves into a delta rarefaction-shock and then into a delta double-rarefaction as first one cloud and then the other is fully accreted into the singularity. A high-resolution finite volume method that captures this behavior is also presented and numerical results shown.

Keywords: Pressureless gas; sticky particles; dust clouds; delta shocks; numerical method.

1. Introduction

In one space dimension the pressureless gas equations are

$$\begin{aligned} \rho_t + (\rho u)_x &= 0 \\ (\rho u)_t + (\rho u^2)_x &= 0 \end{aligned} \tag{1}$$

where $\rho(x,t)$ is the dust density and $u(x,t)$ the velocity. These equations and some aspects of their solutions have been extensively studied, e.g., [2–5, 7, 8, 12]. The system (1) expresses the conservation of mass and momentum in the absense of pressure forces. It is not strictly hyperbolic and the Jacobian matrix is not diagonalizable. In order to derive meaningful single-valued weak solutions to these equations we will assume that the solution desired is the limit as $a \to 0$ of the solution to the isothermal equations

$$\begin{aligned} \rho_t + (\rho u)_x &= 0 \\ (\rho u)_t + (\rho u^2 + a^2\rho)_x &= 0 \end{aligned} \tag{2}$$

with a pressure given by the isothermal equation of state

$$p(\rho) = a^2\rho. \tag{3}$$

A different equation of state (e.g., for isentropic flow) could equally well be used and a corresponding limit taken (as is done in [6], for example). What is crucial for the analysis presented here (and most other analyses of (1)) is that by "pressureless" we really mean the limit as a parameter in the equation of state such as a in (3) vanishes. This is a singular limit since typically $\rho \to \infty$ at some points in the solution, which then contains delta function singularities.

The equation of state (3) is particularly simple to work with since the sound speed a is constant. The system (2) is strictly hyperbolic and has well-understood weak solutions that may contain shock waves with finite jump discontinuities. As $a \to 0$, however, shock waves in the two families may coalesce into "delta shocks" that consist of a finite jump coupled with delta function singularities in mass and momentum.

One case that has been extensively studied is the Riemann problem with data

$$\rho(x,0) = \begin{cases} \rho_l & \text{if } x < 0, \\ \rho_r & \text{if } x > 0, \end{cases} \qquad u(x,0) = \begin{cases} u_l & \text{if } x < 0, \\ u_r & \text{if } x > 0, \end{cases} \tag{4}$$

with $u_l > u_r$. This can be viewed as modeling the collision of two semi-infinite clouds of dust from the moment of impact onwards. If this data is used for the isothermal equations (2) with $a > 0$ then two shock waves result from the collision with a state of elevated mass and momentum between. As $a \to 0$ these two shocks coalesce into a delta shock whose dynamics are easy to determine, as reviewed in Sec. 2.

The system (1) is sometimes said to model "sticky particles" (e.g., [5]) rather than "pressureless dust" in order to reflect the fact that the colliding dust clouds cannot interpenetrate but instead the dust particles stick together to form a point mass of increasing magnitude at the delta shock. This is a reflection of our assumption that it is the $a \to 0$ limit of vanishing pressure we desire. Other truly pressureless models might allow interpenetration of the clouds, a crossing of the characteristics (particle paths in this case), and multivalued solutions.

One goal of this paper is to extend previous delta shock analysis to cases where one or both of these dust clouds has finite length initially and is surrounded by vacuum. Then the delta shock eventually evolves into a "delta rarefaction-shock" or a "delta double-rarefaction", which are the limiting cases of rarefaction-shock and double-rarefaction solutions to the isothermal equations as described in Secs. 3 and 4. An understanding of these solutions provides some additional insight into the structure of general solutions to (1).

A second goal is to present a numerical method for solving (1) that robustly handles delta waves and vacuum states (Sec. 5) and can capture the exact solution derived in Sec. 4. As might be expected, delta shocks are captured more sharply than delta rarefactions.

This work was initially motivated by the study of dusty gas models in which a pressureless model for dust density and momentum is coupled to the Euler equations for a gas in which the dust is suspended. The two sets of equations are coupled through source terms modeling drag and heat transfer. This is a reasonable model for dilute dust concentrations but requires solving system (1) as one component of the solution. This is being explored further with M. Pelanti in the context of ash dispersal from volcanic eruptions.

2. Solution to the Riemann Problem

We first review the well-known delta shock solution to the Riemann problem (4). If $u_l < u_r$ then the two dust clouds move apart with a vacuum state between. We are interested in the case $u_l > u_r$, in which case the solution has the form

$$\begin{aligned} \rho(x,t) &= \rho_l + (\rho_r - \rho_l)H(x - X(t)) + D_1(t)\delta(x - X(t)) \\ \rho(x,t)u(x,t) &= \rho_l u_l + (\rho_r u_r - \rho_l u_l)H(x - X(t)) + D_2(t)\delta(x - X(t)), \end{aligned} \tag{5}$$

where $H(x)$ is the Heaviside function, $\delta(x)$ is the delta function, $X(t)$ is the delta shock location, and $D_1(t), D_2(t)$ are the mass and momentum concentrated at the delta shock, respectively. For the Riemann problem, the delta shock moves at constant velocity, $X(t) = \hat{u}t$, where

$$\hat{u} = \frac{\sqrt{\rho_l}u_l + \sqrt{\rho_r}u_r}{\sqrt{\rho_l} + \sqrt{\rho_r}}, \tag{6}$$

with linearly increasing strength

$$\boxed{\begin{aligned} D_1(t) &= [\rho_l(u_l - \hat{u}) + \rho_r(\hat{u} - u_r)]t, \\ D_2(t) &= [\rho_l u_l(u_l - \hat{u}) + \rho_r u_r(\hat{u} - u_r)]t. \end{aligned}} \tag{7}$$

One way to derive this result is by solving the Riemann problem for (2) with $a > 0$ and taking the limit $a \to 0$. Alternatively, it can be derived directly from conservation of mass and momentum. The dust initially lying between $-1 < x < 1$ at $t = 0$ will be compressed to the interval $-1 + u_l t < x < 1 + u_r t$ for small $t > 0$ with density ρ_l for $-1 + u_l t < x < \hat{u}t$, density ρ_r for $\hat{u}t < x < 1 + u_r t$, and the concentrated mass $D_1(t)$ at some location $\hat{u}t$. Conservation of mass gives

$$\rho_l + \rho_r = \rho_l(\hat{u}t - (-1 + u_l t)) + \rho_r(1 + u_r t - \hat{u}t) + D_1(t).$$

Solving for $D_1(t)$ and considering conservation of momentum in the same manner yields (7). From these we can solve for the propagation speed $\hat{u}$ as the ratio of momentum to mass in the delta shock,

$$\boxed{\hat{u} = \frac{D_2(t)}{D_1(t)}.} \tag{8}$$

Using expressions (7) in this equation and solving for $\hat{u}$ yields (6).

Note that the expression (6) for the delta shock speed is what is called the "Roe-averaged velocity" in the theory of approximate Riemann solvers often used in numerical methods for gas dynamics. Roe [13] proposed approximating a nonlinear problem such as (2) by a linearized system

$$q_t + \hat{A} q_x = 0$$

where the matrix $\hat{A}$ depends on the Riemann data and satisfies the condition

$$\hat{A}(q_r - q_l) = f(q_r) - f(q_l). \tag{9}$$

For system (2), the matrix $\hat{A}$ can be taken to be the Jacobian matrix for the nonlinear problem evaluated at density $\bar{\rho} = \frac{1}{2}(\rho_l + \rho_r)$ and velocity $\hat{u}$ given by (6), as shown in [9], for example. The eigenvalues of this matrix are $\hat{u} \pm a$ and the solution to this linear Riemann problem tends, as $a \to 0$, to the same delta-shock solution as obtained from the nonlinear system. Matter accumulates in the delta shock at the correct rate for this to be true because Roe's condition (9) guarantees conservation. Since the Roe-averaged speed $\hat{u}$ is independent of a, it follows that this must be the speed of the delta-shock that is obtained in the limit $a \to 0$.

3. Collision of a Finite Cloud with a Semi-Infinite Cloud

Now consider the initial data

$$\rho(x,0) = \begin{cases} 0 & \text{if } x < -w_l, \\ \rho_l & \text{if } -w_l < x < 0, \\ \rho_r & \text{if } x > 0, \end{cases} \qquad u(x,0) = \begin{cases} 0 & \text{if } x < -w_l, \\ u_l & \text{if } -w_l < x < 0, \\ u_r & \text{if } x > 0, \end{cases} \tag{10}$$

again with $u_l > u_r$. At time $t = 0$, a dust cloud of length w_l collides with the semi-infinite cloud for $x > 0$. Initially a delta shock propagates as in the Riemann solution of Sec. 2, until the time

$$\text{T1 :=} \quad \boxed{T = \frac{w_l}{u_l - \hat{u}}} \tag{11}$$

at which the left edge of the cloud propagating with speed u_l reaches the delta shock (see Fig. 1). At this point the entire left cloud has been accreted into the delta wave, which then continues to propagate into the semi-infinite cloud accreting additional mass and momentum. But now the accreted matter all comes from the slower moving right cloud and is no longer balanced by accretion of additional faster moving matter from the left cloud, and so the delta wave begins to decelerate.

Let $X(t)$ be the position of the propagating delta wave, with $X(t) = \hat{u}t$ for $0 \le t \le T$. For $t > T$ we can obtain an ODE for $X(t)$ that reveals the dynamics. From Fig. 1 we see that the total mass and momentum accreted into the delta wave by time $t > T$ is

$$\boxed{\begin{aligned} D_1(t) &= w_l \rho_l + (X(t) - u_r t)\rho_r, \\ D_2(t) &= w_l \rho_l u_l + (X(t) - u_r t)\rho_r u_r, \end{aligned}} \tag{12}$$

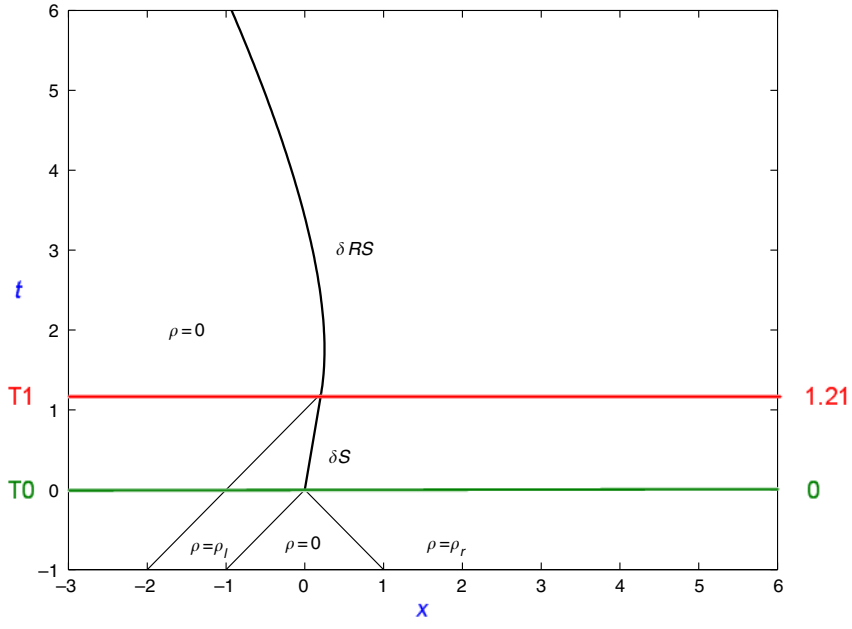

Fig. 1. Collision of a finite dust cloud of length $w_l = 1$ with a semi-infinite dust cloud, shown in the x-t plane. Note that the Riemann problem discussed in the text starts at time $t = 0$ when the two clouds collide. The heavy line shows the delta shock (indicated by δS) and the delta rarefaction-shock (δRS) that arise in the solution, for $0 < t < T$ and $t > T$, respectively. Here $T \approx 1.21$.

and the delta wave velocity is given by the ratio

$$X'(t) = \frac{w_l \rho_l u_l + (X(t) - u_r t)\rho_r u_r}{w_l \rho_l + (X(t) - u_r t)\rho_r}. \tag{13}$$

Solving this differential equation is simplified by introducing

$$W(t) = X(t) - u_r t,$$

so that $W'(t) = X'(t) - u_r$. Using (13) and simplifying gives

$$W'(t) = \frac{w_l \rho_l (u_l - u_r)}{w_l \rho_l + W(t)\rho_r} \tag{14}$$

with the initial condition

$$W(T) = (\hat{u} - u_r)T. \tag{15}$$

Solving this, we obtain

$$X(t) = u_r t - w_l R + \sqrt{2 w_l R (u_l - u_r)t + w_l^2 (R^2 - R)}, \tag{16}$$

where

$$R = \frac{\rho_l}{\rho_r}.$$

Note that $X'(t) > u_r$ for all $t > 0$ but $X'(t) \to u_r$ as $t \to \infty$. The speed of the propagating delta wave asymptotes to u_r as additional matter with speed u_r continues to be accreted.

For $t > T$ the delta wave has vacuum to the left and the cloud with density ρ_r to the right. It is not simply a "delta shock" at this point. Going back to the isothermal equations, we find that the structure for $a > 0$ would consist of a thin region bounded by a 2-shock propagating into the semi-infinite cloud and a 1-rarefaction propagating into the vacuum state. The $a \to 0$ limiting solution might be called a "delta rarefaction-shock" in this case, and is denoted by δRS in Fig. 1. If the cloud on the right were of finite extent instead of the cloud on the left, then a delta shock-rarefaction would arise once the right cloud is entirely accreted.

4. Collision of Two Finite Clouds

If the right cloud also has finite extent w_r initially with vacuum for $x > w_r$, then eventually all of this matter will also be accreted into the delta function. This happens at time T_2 satisfying

$$X(T_2) = w_r + u_r T_2, \tag{17}$$

from which we find that

$$T_2 = \frac{w_r^2 + 2w_l w_r R + w_l^2 R}{2w_l R(u_l - u_r)}. \tag{18}$$

For $t > T_2$ the solution simply consists of a delta function in vaccum that has accumulated all the matter, and hence has mass and momentum

$$\begin{aligned} D_1(t) &= \rho_l w_l + \rho_r w_r, \\ D_2(t) &= \rho_l u_l w_l + \rho_r u_r w_r. \end{aligned} \tag{19}$$

The delta function now propagates at constant speed

$$X'(t) = D_2(t)/D_1(t) = \frac{\rho_l u_l w_l + \rho_r u_r w_r}{\rho_l w_l + \rho_r w_r}. \tag{20}$$

If we consider the isothermal equations with $a > 0$, a thin zone with large mass and momentum surrounded by vacuum would result in two rarefaction waves, and so this structure might be called a "delta double-rarefaction", and is denoted by δRR in Fig. 2. Here we have assumed the cloud on the left is fully accreted before the cloud on the right. The opposite case can be handled similarly.

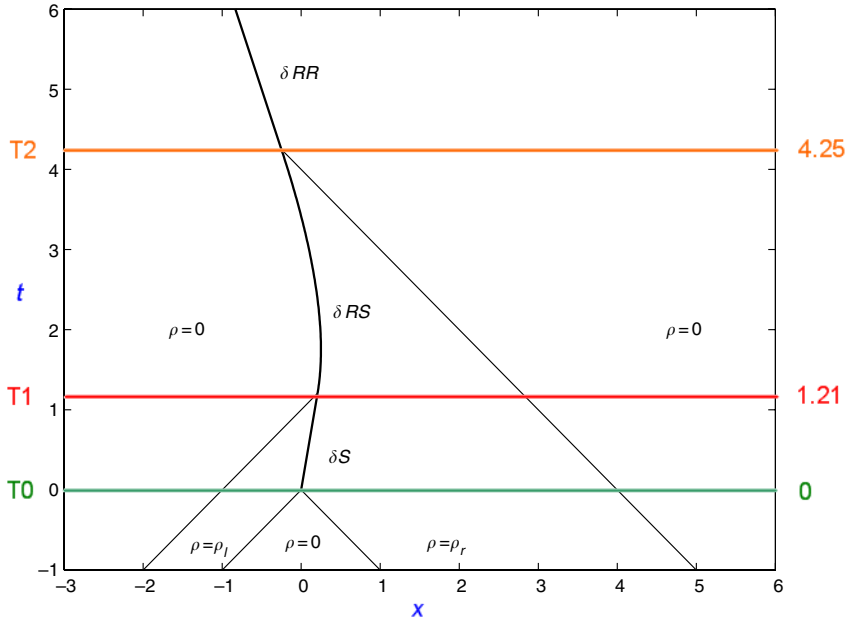

Fig. 2. Collision of a dust cloud of length $w_l = 1$ with a dust cloud of length $w_r = 4$, shown in the x-t plane. Note that the Riemann problem discussed in the text starts at time $t = 0$ when the two clouds collide. The heavy line shows the delta shock (indicated by δS), the delta rarefaction-shock (δRS), and the delta double-rarefaction (δRR). Here $T \approx 1.21$ and $T_2 \approx 4.25$.

5. A Numerical Method

In order to solve the pressureless gas equations numerically, a variant of the high-resolution wave-propagation algorithm described in [10] and [11] is used that appears to work well in the presence of delta waves and vacuum states. This finite volume method for the system $q_t + f(q)_x = 0$ given by (1) takes the form

$$Q_i^{n+1} = Q_i^n - \frac{\Delta t}{\Delta x}(F_{i+1/2} - F_{i-1/2}) - \frac{\Delta t}{\Delta x}(\tilde{F}_{i+1/2} - \tilde{F}_{i-1/2}). \tag{21}$$

The numerical flux $F_{i-1/2}$ is the Godunov flux at the interface $x_{i-1/2}$ that results from solving the Riemann problem between states Q_{i-1}^n and Q_i^n, as described below. The correction flux $\tilde{F}_{i-1/2}$ models terms needed to obtain second-order accuracy on smooth solutions, with limiters added to avoid spurious oscillations.

The Godunov flux. If $u_{i-1} < 0 < u_i$ then the dust is moving away from the interface at $x_{i-1/2}$ on both sides, leaving vacuum between, and so

$$F_{i-1/2} = 0 \qquad \text{if } u_{i-1} < 0 < u_i. \tag{21.5}$$

Otherwise, we compute

$$\hat{u}_{i-1/2} = \frac{\sqrt{\rho_{i-1}}u_{i-1} + \sqrt{\rho_i}u_i}{\sqrt{\rho_{i-1}} + \sqrt{\rho_i}}, \tag{22}$$

and set

$$F_{i-1/2} = \begin{cases} f(Q^n_{i-1}) & \text{if } \hat{u}_{i-1/2} > 0 \\ \frac{1}{2}(f(Q^n_{i-1}) + f(Q^n_i)) & \text{if } \hat{u}_{i-1/2} = 0 \\ f(Q^n_i) & \text{if } \hat{u}_{i-1/2} < 0. \end{cases} \tag{23}$$

The case $\hat{u}_{i-1/2} = 0$ is special since a delta shock should be forming right at the interface $x_{i-1/2}$ in this case, which is distributed between the two neighboring cells.

The correction terms. When solving a strictly hyperbolic system of two conservation laws with two distinct waves in the Riemann solution, the correction flux is generally defined as

$$\tilde{F}_{i-1/2} = \frac{1}{2}\sum_{p=1}^{2} |s^p_{i-1/2}| \left(1 - \frac{\Delta t}{\Delta x}|s^p_{i-1/2}|\right) \widetilde{\mathcal{W}}^p_{i-1/2}, \tag{24}$$

where $s^p_{i-1/2} (p = 1, 2)$ are the two wave speeds and $\widetilde{\mathcal{W}}^p_{i-1/2}$ are limited versions of the waves $\mathcal{W}^p_{i-1/2}$ that come from solving the Riemann problem. These waves are defined in such a way that

$$Q^n_i - Q^n_{i-1} = \mathcal{W}^1_{i-1/2} + \mathcal{W}^2_{i-1/2}.$$

See [10] and [11] for more details. For the pressureless gas equations the solution consists of two waves if $u_{i-1} < u_i$ (with vacuum state between) but only a single delta shock if $u_{i-1} > u_i$. One numerical approach would be to replace the system (1) by the isothermal system (2) with some small value of $a > 0$. This gives a strictly hyperbolic system with two distinct waves in the Riemann solution. However, when $u_{i-1} > u_i$ the two waves will each have large amplitude and opposite sign, corresponding to a jump up from Q^n_{i-1} to a large intermediate value (approximating the delta shock that forms in the $a = 0$ limit) followed by a large jump back down to state Q^n_i. When these large waves are used in the correction terms, poor results are typically obtained.

Better results are obtained by coalescing these two waves into a single wave with strength $Q^n_i - Q^n_{i-1}$ except in the case $u_{i-1} < 0 < u_i$, in which case the two distinct waves propagate in different directions. This suggests the following algorithm:

If $u_{i-1} < 0 < u_i$, set

$$\mathcal{W}^1_{i-1/2} = -Q^n_{i-1}, \qquad s^1_{i-1/2} = u_{i-1}$$
$$\mathcal{W}^2_{i-1/2} = Q^n_i, \qquad s^2_{i-1/2} = u_i.$$

Otherwise, compute $\hat{u}_{i-1/2}$ by (22) and use:

$$\begin{aligned} \text{if } \hat{u}_{i-1/2} < 0: \quad & \mathcal{W}^1_{i-1/2} = Q^n_i - Q^n_{i-1}, && s^1_{i-1/2} = \hat{u}_{i-1/2} \\ & \mathcal{W}^2_{i-1/2} = 0, && s^2_{i-1/2} = \hat{u}_{i-1/2} \\ \text{if } \hat{u}_{i-1/2} \geq 0: \quad & \mathcal{W}^1_{i-1/2} = 0, && s^1_{i-1/2} = \hat{u}_{i-1/2} \\ & \mathcal{W}^2_{i-1/2} = Q^n_i - Q^n_{i-1}, && s^2_{i-1/2} = \hat{u}_{i-1/2} \end{aligned}$$

Limiters are then applied to the waves in order to define the waves $\widetilde{\mathcal{W}}^p_{i-1/2}$ used in the correction terms.

This method has been found to work well for test problems with data of the form considered in this paper, but does not work well for other test problems where the velocity u changes sign in regions where the density is smoothly varying. This is due to an inconsistency of the finite volume formulation of these equations near sonic points, as has also been observed with other methods (see [2] and [4] for some discussion and another numerical approach based on kinetic methods).

A variant of this algorithm has been found to be more robust and accurate in general. The correction terms are based on waves defined from splitting the flux difference $f(Q^n_i) - f(Q^n_{i-1})$ rather than splitting $Q^n_i - Q^n_{i-1}$. This *f-wave approach* is developed in [1] and briefly discussed in [11].

In place of (24), the correction terms are defined by

$$\tilde{F}_{i-1/2} = \frac{1}{2}\sum_{p=1}^{2} \operatorname{sgn}(s^p_{i-1/2}) \left(1 - \frac{\Delta t}{\Delta x}|s^p_{i-1/2}|\right) \widetilde{\mathcal{Z}}^p_{i-1/2}, \tag{25}$$

where

$$f(Q^n_i) - f(Q^n_{i-1}) = \mathcal{Z}^1_{i-1/2} + \mathcal{Z}^2_{i-1/2}.$$

The algorithm for defining this splitting is exactly analogous to the one presented above:

If $u_{i-1} < 0 < u_i$, set

$$\mathcal{Z}^1_{i-1/2} = -f(Q^n_{i-1}), \qquad s^1_{i-1/2} = u_{i-1}$$
$$\mathcal{Z}^2_{i-1/2} = f(Q^n_i), \qquad s^2_{i-1/2} = u_i$$

Otherwise, compute $\hat{u}_{i-1/2}$ by (22) and use:

$$\begin{aligned}
\text{if } \hat{u}_{i-1/2} < 0: \quad & \mathcal{Z}^1_{i-1/2} = f(Q^n_i) - f(Q^n_{i-1}), && s^1_{i-1/2} = \hat{u}_{i-1/2} \\
& \mathcal{Z}^2_{i-1/2} = 0, && s^2_{i-1/2} = \hat{u}_{i-1/2} \\
\text{if } \hat{u}_{i-1/2} \geq 0: \quad & \mathcal{Z}^1_{i-1/2} = 0, && s^1_{i-1/2} = \hat{u}_{i-1/2} \\
& \mathcal{Z}^2_{i-1/2} = f(Q^n_i) - f(Q^n_{i-1}), && s^2_{i-1/2} = \hat{u}_{i-1/2}
\end{aligned}$$

Limiters are then applied to these waves in the usual manner, by comparing each wave to the corresponding wave in the upwind direction. In order to minimize undershoots near vacuum states, a componentwise limiter has been used in which each component of the wave is limited by applying the minmod limiter to this wave and its upwind neighbor. Moreover, if the addition of the limited waves results in a value of the density ρ_i in some cell being negative, then the waves $\widetilde{\mathcal{W}}^p_{i-1/2}$ and $\widetilde{\mathcal{W}}^p_{i+1/2}$ are further limited to the value 0, i.e., no correction waves are used in this cell.

Vacuum states in the initial data were replaced by a density $\rho = 10^{-20}$. Some negative undershoots are observed in the computation, and these values are replaced by this density $\rho = 10^{-20}$, but for the test problem presented below these undershoots were in the order of -10^{-25} or smaller.

Figures 3 and 4 show numerical results obtained for a test problem of the form discussed in Sec. 4. The initial data is

$$\rho(x,-1) = \begin{cases} 2 & \text{if } -2 < x < -1, \\ 1 & \text{if } 1 < x < 5, \\ 0 & \text{otherwise.} \end{cases} \qquad u(x,-1) = \begin{cases} 1 & \text{if } -2 < x < -1, \\ -1 & \text{if } 1 < x < 5, \\ 0 & \text{otherwise.} \end{cases} \tag{26}$$

Two dust clouds of length 1 and 4 are initialized at time $t = -1$ and collide at time $t = 0$, as shown in the x-t plane in Fig. 2.

Figures 3 and 4 show the results at a sequence of 8 times. Note that the two clouds collide at time $t = 0$, the left cloud is fully accreted into the delta wave at time $T \approx 1.21$ and the right cloud is fully accreted at time $T_2 \approx 4.25$. The thick vertical line in plots for $t > 0$ indicates the true position of the delta wave, which is

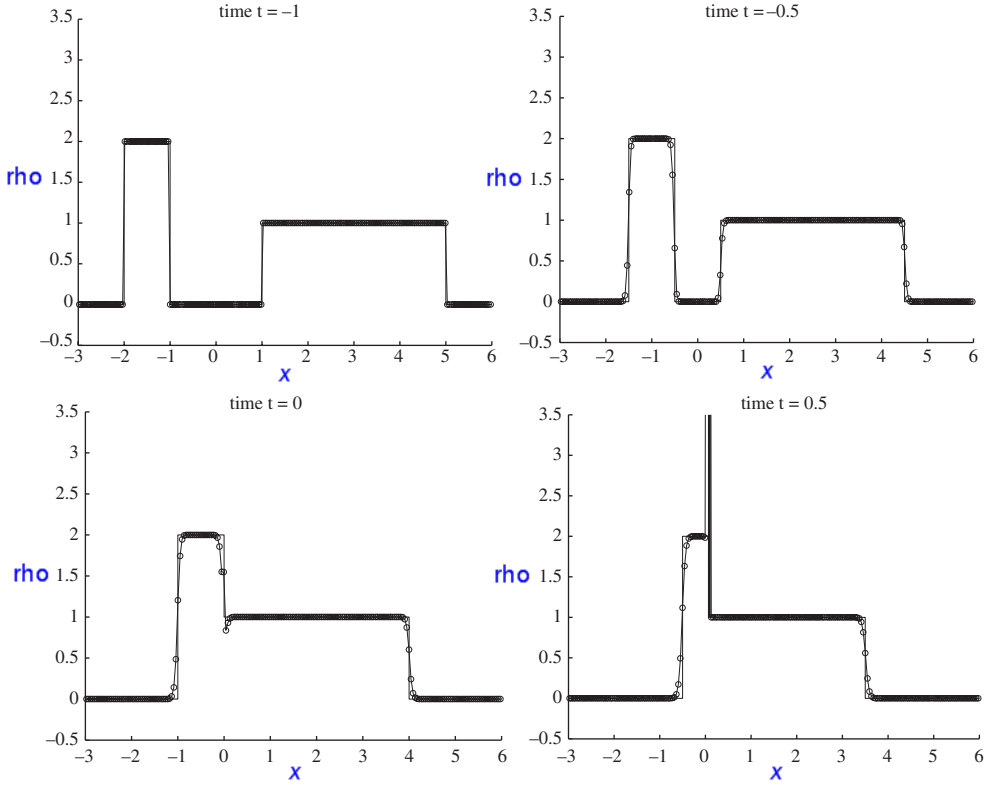

Fig. 3. Numerical solution of the problem illustrated in Fig. 2.

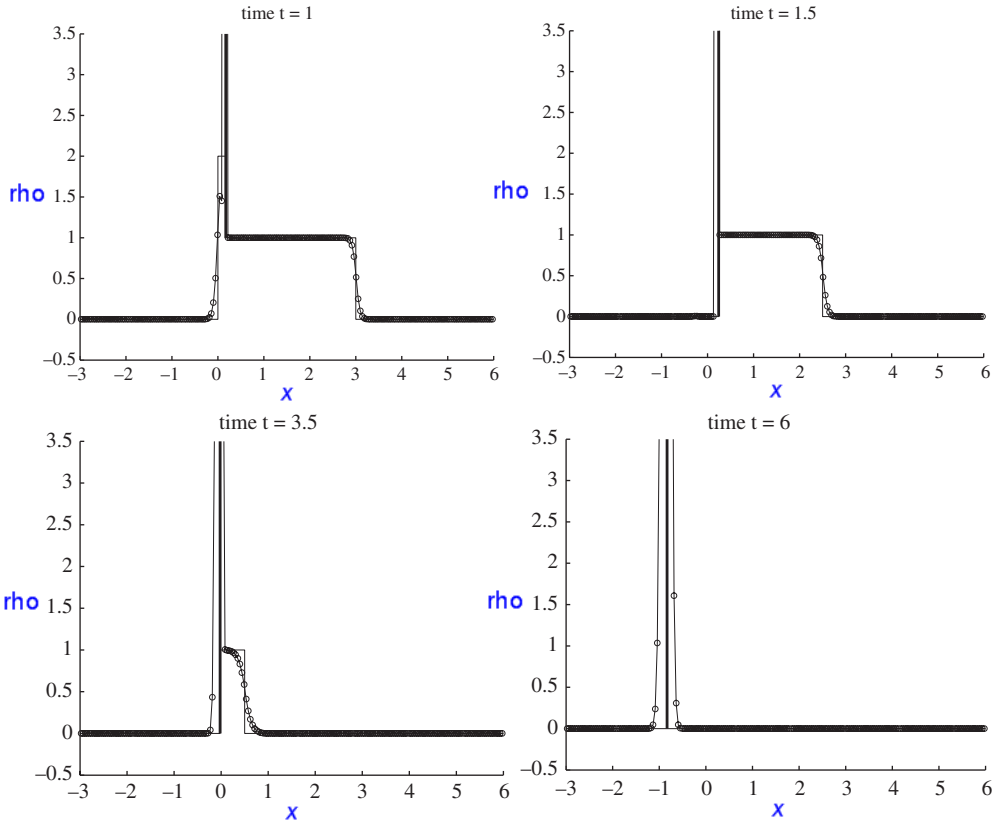

Fig. 4. Numerical solution of the problem illustrated in Fig. 2, continued.

a delta function singularity. The numerical results give a smeared representation of this wave, but one that is located in the correct position. The figures have all been plotted on the same vertical scale with peak values of the computed density clipped near the region of the delta functions. At times $t = 0.5,\ 1.0,\ 1.5$ there are only 2 grid values not shown and the peak density values were approximately 20.2, 44.0, and 58.2, respectively. The total mass is correct in each case since the method is conservative (except for the negligible errors due to resetting the negative densities at undershoots).

By time $t = 3.5$ the delta rarefaction-shock is becoming more smeared out on the rarefaction side. Five grid values have been clipped off in the zoomed view and the density peak is down to 51.6 at this time, even though the strength of the true delta wave has increased. The total mass is still correct but has been smeared over more grid points. By time $t = 6$ all the mass is concentrated in a single delta double-rarefaction which has been smeared over more points both to the left and the right. In addition to the points shown

in the zoomed view, another 7 grid points have been clipped off and the peak density is 29.8.

6. Conclusions

The delta shock that arises in the Riemann solution for two colliding dust clouds evolves into a delta rarefaction-shock when one cloud has been fully accreted and then into a delta double-rarefaction when both clouds have been fully accreted. A numerical method has been presented and used to confirm the analytic expressions obtained in this paper and to illustrate the potential for computing such solutions numerically. The delta rarefaction-shock and delta double-rarefaction adjacent to vacuum states can be captured with this method, though not as sharply as a simple delta shock.

Acknowledgments

This work was supported in part by DOE grant DE-FC02-01ER25474 and NSF grant DMS-0106511.

I also gratefully acknowledge the support and hospitality of the Isaac Newton Institute for Mathematical Sciences at the University of Cambridge, where part of this research was performed in 2003, during the Semester Program "Nonlinear Hyperbolic Waves in Phase Dynamics and Astrophysics" organized by C. M. Dafermos, P. G. LeFloch, and E. Toro.

References

[1] D. Bale, R. J. LeVeque, S. Mitran and J. A. Rossmanith, A wave-propagation method for conservation laws and balance laws with spatially varying flux functions, *SIAM J. Sci. Comput.* **24** (2002) 955–978.

[2] F. Bouchut, On zero pressure gas dynamics, in *Advances in Kinetic Theory and Computing*, ed. B. Perthame, Ser. Adv. Math. Appl. Sci., Vol. 22 (World Scientific, 1994), pp. 171–190.

[3] F. Bouchut and F. James, Duality solutions for pressureless gases, monotone scalar conservation laws, and uniqueness, *Commun. Math. Phys.* **24** (1999) 2173–2189.

[4] F. Bouchut, S. Jin and X. Li, Numerical approximations of pressureless and isothermal gas dynamics, *SIAM J. Numer. Anal.* **41** (2003) 135–158.

[5] Y. Brenier and E. Grenier, Sticky particles and scalar conservation laws, *SIAM J. Numer. Anal.* **35** (1998) 2317–2328.

[6] G.-Q. Chen and H. Liu, Formation of δ-shocks and vacuum states in the vanishing pressure limit of solutions to the Euler equations for isentropic fluids, *SIAM J. Math. Anal.* **34** (2003) 925–938.

[7] W. E, Y. G. Rykov and Y. G. Sinai, Generalized variational principles, global weak solutions and behavior with random initial data for systems of conservation laws arising in adhesion particle dynamics, *Commun. Math. Phys.* **177** (1996) 349–380.

[8] F. Huang and Z. Wang, Well posedness for pressureless flow, *Commun. Math. Phys.* **222** (2001) 117–146.

[9] R. J. LeVeque, *Numerical Methods for Conservation Laws* (Birkhäuser-Verlag, 1990).

[10] R. J. LeVeque, Wave propagation algorithms for multi-dimensional hyperbolic systems, *J. Comput. Phys.* **131** (1997) 327–353.
[11] R. J. LeVeque, *Finite Volume Methods for Hyperbolic Problems* (Cambridge University Press, 2002).
[12] J. Li and T. Zhang, On the initial-value problem for zero-pressure gas dynamics, in *Proc. 7'th Intl. Conf. on Hyperbolic Problems*, ed. R. Jeltsch (Birkhäuser Verlag, 1998), pp. 629–640.
[13] P. L. Roe, Approximate Riemann solvers, parameter vectors, and difference schemes, *J. Comput. Phys.* **43** (1981) 357–372.